

Visual servoing of a class of under-actuated dynamic rigid-body systems

T. Hamel

Cemif, Université d'Evry,
40 rue du Pelvoux,
91020 Courcouronnes, FRANCE.
email: thamel@iup.univ-evry.fr

R. Mahony

Dep. of Elec. and Comp. Sys. Eng.
Monash University, Clayton, Victoria,
3800, AUSTRALIA.
email: mahony@ieee.org

Abstract

A new image-based control strategy for visual servoing is presented. The proposed control design addresses visual servoing of 'eye-in-hand' type systems and treats the camera motion as rigid-body dynamics that are positioned relative to an observed visual target. The proposed design is applicable to a class of under-actuated dynamic systems that include idealized models of mobile robotic vehicles such as helicopters, aeroplanes, etc. The proposed design is motivated by a theoretical analysis of the dynamic equations of motion of an under-actuated rigid body and exploits passivity-like properties of these dynamics to derive a Lyapunov control algorithm using robust backstepping techniques.

1 Introduction

Visual feedback control algorithms have been extensively developed in the robotics field over the last ten years. [1, 2]. Most visual servoing techniques [1, 3] rely on an accurate knowledge of the target and require that there is sufficient information present in the target to ensure that the task representation is non-degenerate [4]. This condition reduces to a mathematical requirement that there is a diffeomorphism between task space and the degrees of liberty of the system considered. Existing image-based visual servoing algorithms exploit this mapping explicitly, using the Jacobian of the task representation map to represent control authority directly in the task space. Kinematic, or static state, feedback control is then used to regulate an error function measured directly in the task space and derived from the control objective. There are two principal disadvantages of this approach: Firstly, the method relies on accurate knowledge of the target geometry to derive the task representation map. Secondly, this approach does not generalize well to the case where the dynamics of the system are important [5] or when the system is under-actuated. Most existing generalizations of classical visual servoing techniques exploit a high gain or computed torque feedback to make a dynamic reduction of the system to a controllable kinematic model for which the visual servoing task may be solved directly

(cf. [2] and references therein). The full dynamic response of a system is commonly ignored in the design of visual servo systems and closed-loop performance may be severely limited to ensure that the dynamic reduction is valid. Corke and Good [5] have considered some of the issues that arise when the dynamic reduction is not truly valid. Recently Kelly [6] has explored a more nonlinear aspect of the system dynamics, and presented an asymptotically stable method for position regulation for fixed-camera visual servoing. Recent work by Zergeroglu *et al.* [7] has used robust backstepping techniques to deal with the full dynamics of a planar robot in a visual servoing context, while Maruyama *et al.* [8] have investigated dissipative control strategies. The difficulties associated with controlling an under-actuated system have received even less attention. Ostrowski and Zhang [9] have been working on the visual servoing problem using a Lagrangian representation of the system dynamics and consider under-actuated and non-holonomic systems. Shakernia *et al.* [10] are also considering visual servoing of dynamic system (motivated by control of UAVs) based on the direct determination of the 'planar differential essential matrix' that provides kinematic state information directly from the image data and allows one to apply state-space nonlinear control design techniques. Finally we mention the growing interest in developing vision based control algorithms based on biological insights [11].

In this paper we develop a paradigm of visual servoing for under-actuated dynamic systems which operate without accurate target information. The problem considered is that of 'eye-in-hand' servoing where the motion of the camera (rigidly attached to the robot) is regulated relative to the environment. An image based error criterion is used in preference to a position based system that would necessitate pose reconstruction and suffer the consequent robustness issues associated with such procedures. The proposed approach is motivated by a theoretical analysis of the dynamic equations of motion of a rigid body and exploits structural passivity-like properties of these dynamics to derive a Lyapunov control algorithm using robust backstepping techniques. This approach overcomes some of the difficulties associated with the highly non-linear

coupling associated with the image-based approach at the expense of requiring additional measurements of certain dynamic states of the system.

2 Visual Dynamics of a Point Target and Passivity-Like Properties.

In this section a general dynamic model of a rigid body evolving in \mathbb{R}^3 is presented. These dynamics are then used to derive the dynamics of a stationary target in the image plan.

Denote the body of the rigid object by the letter \mathbf{A} . Let $\mathcal{I} = \{E_x, E_y, E_z\}$ denote a right-hand inertial frame such that E_z denotes the vertical direction downwards into the earth. Let the vector $\xi = (x, y, z)$ denote the position of the centre of mass of the object in the frame \mathcal{I} relative to a fixed origin $0 \in \mathcal{I}$. Let $\mathcal{A} = \{E_1^a, E_2^a, E_3^a\}$

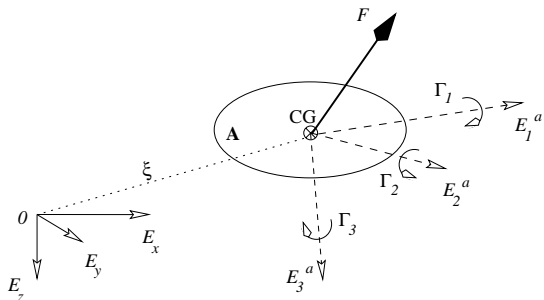


Figure 1: Rigid Body with Force and Torque Control.

be a (right-hand) body fixed frame for \mathbf{A} . The orientation of the rigid body is given by a rotation $R : \mathcal{A} \rightarrow \mathcal{I}$, where $R \in SO(3)$ is an orthogonal rotation matrix.

Let $X := R^T \xi \in \mathbb{R}^3$ denote the position of the body (relative to the origin $0 \in \mathcal{I}$) expressed in the body fixed frame $X \in \mathcal{A}$. Let $V \in \mathcal{A}$ denote the linear velocity and $\Omega \in \mathcal{A}$ denote the angular velocity of the rigid object both expressed in the body fixed frame. Let m denote the mass of the rigid object and let $\mathbf{I} \in \mathbb{R}^{3 \times 3}$ denote the constant inertia matrix around the centre of mass (expressed in the body fixed frame \mathcal{A}). Newton's equations of motion yield the following dynamic model for the motion of a rigid object:

$$\dot{X} = -\Omega \times X + V \quad (1)$$

$$m\dot{V} = -m\Omega \times V + F \quad (2)$$

$$\dot{R} = R \text{sk}(\Omega), \quad (3)$$

$$\mathbf{I}\dot{\Omega} = -\Omega \times \mathbf{I}\Omega + \Gamma. \quad (4)$$

where $F \in \mathcal{A}$ combines all the external linear forces acting on the rigid object (including gravity) and Γ does the same for all torques. The notation $\text{sk}(\Omega)$ denotes the skew-symmetric matrix such that $\text{sk}(\Omega)v = \Omega \times v$ for the vector cross-product \times and any vector $v \in \mathbb{R}^3$.

In earlier work [12] the cascade structure of Eqn's 1-4 was exploited to design a full non-linear control algorithm for an idealized model of a helicopter. The main contribution of this paper is to show that a backstepping design for visual servoing may be undertaken by exploiting the structural passivity properties of Eqn's 1-4. By this, we refer to the passivity-like properties (from virtual input to the backstepping error) typical of each iteration of backstepping control designs [13].

To simplify the derivation it is assumed that the camera frame coincides with the body fixed frame. Let P_i for $i = 1, \dots, n$ represent n stationary point targets which are visible to the camera. The points P_i are measured in the body fixed frame $P_i \in \mathcal{A}$. If $\bar{P}_i \in \mathcal{I}$ is the inertial representation of P_i then

$$P_i = R^T (\bar{P}_i - \xi).$$

An key aspect of the proposed design is to use spherical geometry for the camera. The spherical image of a point target observed by the camera is denoted p_i . Assuming (without loss of generality) that the focal length of the camera is $f = 1$, the observed point image p_i may be written

$$p_i = \frac{1}{r_i} P_i. \quad (5)$$

where $r_i = |P_i|$. Define $V_i \in \mathcal{A}$ to be the observed velocity of the target point P_i represented in the camera fixed frame

$$V_i := R^T (\dot{\bar{P}}_i - \dot{\xi}) = -R^T \dot{\xi} = -V$$

The image dynamics of a point target for a spherical camera are

$$\begin{aligned} \dot{p}_i &= \frac{1}{r_i} \dot{P}_i - \frac{d}{dt} \frac{r_i}{r_i^2} P_i \\ &= -\text{sk}(\Omega) p_i + \frac{\pi_{p_i}}{r_i} V, \end{aligned} \quad (6)$$

where $\pi_p = (I_3 - pp^T)$ is the projection $\pi_p : \mathbb{R}^3 \rightarrow T_p S^2$ onto the tangent space of the sphere S^2 at the point $p \in S^2$. These dynamics preserve the important passivity-like behaviour of Eq. 1

$$\frac{d}{dt} p_i^T p_i = p_i^T \frac{\pi_{p_i}}{r_i} V$$

that is the key to applying the proposed control design (cf. the companion paper [14]). This property is only true for the spherical projection (cf. [15] or contact the authors directly)!

3 Image space error criteria for visual servoing

In this section the image space error considered is introduced. The visual servoing task considered is that of positioning a camera relative to a stationary target.

Intuitively, the objective of a visual servoing algorithm in image space is to match the observed image to a known ‘model’ image of the target. Define a set of desired visual features $\{p_1^*, \dots, p_n^*\}$ which correspond to the expected image of the target if the camera were placed in the desired position and orientation. Thus, $\{p_1^*, \dots, p_n^*\}$ are a set of n points on the spherical image plane. The full image space error term is a $3n$ -dimensional vector

$$\delta = \text{vect}(p_i - p_i^*) \in \mathbb{R}^{3n} \quad (7)$$

In classical visual servoing algorithms the desired visual features are chosen to be fixed relative to the body fixed frame. Thus, minimizing δ ensures a particular orientation of the camera relative to the target. *In this paper we choose the desired visual features p_i^* to be fixed relative to the inertial frame.* This ensures a regulation of the position of the camera in the inertial frame relative to the target. Indeed, in order that the desired visual objects p_i^* are stationary in the inertial frame then in the body fixed frame one has

$$\dot{p}_i^* = -\Omega \times p_i^*.$$

The advantage of choosing the desired visual targets to be fixed in the inertial frame is seen when the first order dynamics of the error are computed. Let

$$\Pi := \begin{pmatrix} \frac{1}{r_1}(I_3 - p_1 p_1^T) \\ \vdots \\ \frac{1}{r_n}(I_3 - p_n p_n^T) \end{pmatrix}.$$

The dynamics of δ are

$$\dot{\delta} = \underbrace{\text{diag}(-\text{sk}(\Omega))}_{3n \times 3n} \underbrace{\delta}_{3n \times 1} - \underbrace{\Pi}_{3n \times 3} \underbrace{V}_{3 \times 1} \quad (8)$$

The full visual error δ usually contains more information than the minimum needed to solve the visual servoing problem. It is usual to ‘average’ by combining the data according to some weighted average. The proposed design uses the concept of a combination matrix [1] to reduce the full error δ to a reduced error vector δ_r . By properly choosing the combination matrix, the reduced error is diffeomorphically related to the position of the camera and the structural passivity-like properties of the image dynamics are preserved.

Definition 1 Let $C \in \mathbb{R}^{3 \times 3n}$ be a full rank combination matrix such that,

$$Q := C\Pi > 0 \text{ and } C\text{diag}(\text{sk}(\Omega)) = \text{sk}(\Omega)C; \quad \forall \Omega \in \mathbb{R}^3$$

It is easily verified that C has the form

$$C = [\alpha_1 I \quad \dots \quad \alpha_n I], \quad \alpha_i \geq 0, \quad \forall i = 1, \dots, n$$

Note that $C\Pi = Q > 0$ relies on the fact that $r_i > 0$ and that *the exact value of Q remains unknown!* Some

information on Q is still needed in the form of bounds on its maximal and minimal eigenvalues

$$\lambda_{\min} I_3 < Q < \lambda_{\max} I_3.$$

The bounds λ_{\min} and λ_{\max} may be estimated from over and under bounds on the target range r_i $i = 1, \dots, n$. This is analogous to the depth information that is necessary to existing image based visual servoing algorithms. It is important to note, however, that in the proposed design only rough bounds on *average* target depth need be obtained, while in existing image based algorithms exact depth information is (theoretically) necessary. The bounds λ_{\min} and λ_{\max} chosen govern the range in which the control design undertaken in Section 4 are valid.

The reduced error vector considered is

$$\delta_1 := C\delta \in \mathbb{R}^3. \quad (9)$$

The visual error considered may be interpreted as the vectorial distance between the weighted centroid of the observed image and a fixed inertial direction. A consequence of this choice is that minimising $|\delta_1|$ regulates only the inertial position of the camera and does not regulate the orientation of the camera. To regulate the full pose of the camera it is necessary to introduce secondary control errors. Such a development is well beyond the scope of the present paper. An advantage of using visual centroid information is that the control design will operate without precise target information. This property of the error structure is expected to ensure strong practical robustness of the control design and makes it particularly suitable to be used in practical applications.

4 Control Design Methodology

In this section it is shown how a visual servoing control may be derived based on robust backstepping techniques for an ‘eye-in-hand’ camera with under-actuated rigid body dynamics.

Deriving the reduced vector δ_1 , using the definition of the combination matrix Def. 1 and recalling Eq. 8, yields the following full dynamics of the error δ_1

$$\dot{\delta}_1 = -\text{sk}(\Omega)\delta_1 - QV \quad (10)$$

$$m\dot{V} = -m\Omega \times V + F \quad (11)$$

$$\dot{R} = R\text{sk}(\Omega), \quad (12)$$

$$\mathbf{I}\dot{\Omega} = -\Omega \times \mathbf{I}\Omega + \Gamma. \quad (13)$$

The particular problem considered is that which occurs when the force input F is not fully actuated while full actuation of the torque Γ is available. Particular, when the force input of the under-actuated rigid body may be written

$$F := -u\mathbf{F} + mgR^T e_3 \quad (14)$$

where $\mathbf{F} \in \mathcal{A}$ is an arbitrary unit vector in the body fixed frame representing the fixed orientation of a thruster or actuator that provides a force input, $u \in \mathbb{R}$ is a scalar input representing the thrust or force applied in direction \mathbf{F} and $mgR^T e_3$ is the gravitational force (Section 5 presents the structure for an idealized helicopter). Such an arrangement is at least a generic first approximation for many flying robots. Intuitively, the system may be controlled by using the full torque control to orient the thrust direction \mathbf{F} as required and using u to govern its magnitude as shown below.

Define δ_2 as the difference between the reduced vector δ_1 and the scaled velocity V

$$\delta_2 := \frac{m}{k_1} V - \delta_1 \quad (15)$$

Introducing δ_2 in Eq. 10, taking the time derivative of δ_2 and substituting for Eq. 16, yields

$$\dot{\delta}_1 = -\text{sk}(\Omega)\delta_1 - \frac{k_1}{m} Q \delta_1 - \frac{k_1}{m} Q \delta_2 \quad (16)$$

$$\dot{\delta}_2 = -\text{sk}(\Omega)\delta_2 + \frac{k_1}{m} Q \delta_1 + \frac{k_1}{m} Q \delta_2 + \frac{1}{k_1} F \quad (17)$$

The control design undertaken is based on the well known robust backstepping techniques [13]. Initially we consider only the error dynamics transformation (Eqn's 16 and 17). Define a storage function $S_{1,2}$

$$S_{1,2} = \frac{1}{2} |\delta_1|^2 + \frac{1}{2} |\delta_2|^2 \quad (18)$$

Taking the time derivative of $S_{1,2}$ and substituting for Eqn's 16-17, yields

$$\dot{S}_{1,2} = -\frac{k_1}{m} \delta_1^T Q \delta_1 + \frac{k_1}{m} \delta_2^T Q \delta_2 + \frac{1}{k_1} \delta_2^T F \quad (19)$$

Note that Eq. 19 is independent of the angular velocity Ω .

As discussed in Section 3 the matrix $Q > 0$ is not exactly known, however, the fact that it is positive definite leads to a simple choice of F that would stabilize $S_{1,2}$ if the force F were available as a control input. The virtual control chosen for Eq. 19 is

$$F^v := -\frac{k_1^2 k_2}{m} \delta_2 \quad \text{where } k_2 > \lambda_{\max}. \quad (20)$$

With this choice, one has

$$\dot{\delta}_2 = -\text{sk}(\Omega)\delta_2 + \frac{k_1}{m} Q \delta_1 - \frac{k_1}{m} (k_2 I - Q) \delta_2 + \frac{k_1}{m} k_2 \delta_3 \quad (21)$$

where δ_3 defines the scaled difference between the desired (virtual) and true forces and will form the new error term in the next step of the backstepping procedure,

$$\delta_3 := \frac{m}{k_1^2 k_2} (F - F^v) = \frac{m}{k_1^2 k_2} F + \delta_2. \quad (22)$$

The derivative of the storage function Eq. 19 is

$$\dot{S}_{1,2} = \frac{k_1}{m} \delta_2^T Q \delta_1 - \frac{k_1}{m} \delta_2^T (k_2 I - Q) \delta_2 + \frac{k_1}{m} k_2 \delta_2^T \delta_3 \quad (23)$$

Deriving δ_3 and recalling Eq. 21, yields

$$\begin{aligned} \dot{\delta}_3 &= -\text{sk}(\Omega)\delta_3 + \frac{k_1}{m} Q \delta_1 - \frac{k_1}{m} (k_2 I - Q) \delta_2 + \frac{k_1}{m} k_2 \delta_3 \\ &\quad + \frac{m}{k_1^2 k_2} \left(\dot{F} + \text{sk}(\Omega)F \right) \end{aligned} \quad (24)$$

Following standard backstepping procedures let $(\dot{F} + \text{sk}(\Omega)F)^v$ denote the virtual control used in the next iteration of the backstepping. The full vectorial term $(\dot{F} + \text{sk}(\Omega)F)^v$ is assigned directly rather than dealing explicitly with the dependence on the actual control inputs. This avoids some complications in the general development due to conflicting contributions from both force and torque control inputs. In practice it is a simple matter to compute the actual control inputs from the vectorial control design (cf. §5). The virtual control assigned is

$$\frac{m}{k_1^2 k_2} \left(\dot{F} + \text{sk}(\Omega)F \right)^v := -\frac{(k_1 k_2 + k_3)}{m} \delta_3 \quad (25)$$

The expression for the derivative of δ_3 may now be written

$$\begin{aligned} \dot{\delta}_3 &= -\text{sk}(\Omega)\delta_3 + \frac{k_1}{m} Q \delta_1 - \frac{k_1}{m} (k_2 I - Q) \delta_2 - \frac{k_3}{m} \delta_3 \\ &\quad + \frac{(k_1 k_2 + k_3)}{m} \delta_4. \end{aligned} \quad (26)$$

Here δ_4 is the last error term used in the backstepping procedure defined by

$$\delta_4 := \frac{m^2}{k_1^2 k_2 (k_1 k_2 + k_3)} \left(\dot{F} + \text{sk}(\Omega)F + \frac{\delta_3}{m^2} \right) \quad (27)$$

Let S_3 be a storage function associated with this step of the procedure defined by

$$S_3 = \frac{1}{2} |\delta_3|^2 \quad (28)$$

Taking the derivative of S_3 and recalling Eq. 26 one obtains

$$\begin{aligned} \dot{S}_3 &= \frac{k_1}{m} \delta_3^T Q \delta_1 - \frac{k_1}{m} \delta_3^T (k_2 I - Q) \delta_2 - \frac{k_3}{m} \delta_3^T \delta_3 \\ &\quad + \frac{(k_1 k_2 + k_3)}{m} \delta_3^T \delta_4 \end{aligned} \quad (29)$$

The derivative of δ_4 is

$$\begin{aligned} \dot{\delta}_4 &= \frac{m^2}{k_1^2 k_2 (k_1 k_2 + k_3)} \left(\ddot{F} + \text{sk}(\dot{\Omega})F + \text{sk}(\Omega)\dot{F} \right) - \text{sk}(\Omega)\delta_3 \\ &\quad + \frac{k_1}{m} Q \delta_1 - \frac{k_1}{m} (k_2 I - Q) \delta_2 - \frac{k_3}{m} \delta_3 + \frac{(k_1 k_2 + k_3)}{m} \delta_4 \end{aligned} \quad (30)$$

At this stage the actual control inputs enter into the equations via \ddot{F} and $\dot{\Omega}$ (cf. Eqn's 4 and 14). The exact manner in which the control inputs enter depends on each individual application and the arrangements of thrust etc. that generate the force F . The application discussed in Section 5 indicates the manner in which this calculation is done in practice. It is assumed that the term $m^2 (\ddot{F} + \text{sk}(\dot{\Omega})F)$ may be arbitrarily assigned¹. To achieve the desired control one chooses

$$m^2 (\ddot{F} + \text{sk}(\dot{\Omega})F) = \frac{k_1^2 k_2 (k_1 k_2 + k_3)}{m} (m \text{sk}(\Omega) \delta_3 - k_1 k_2 \delta_3 - (k_1 k_2 + k_3 + k_4) \delta_4) - m^2 \text{sk}(\Omega) \dot{F} \quad (31)$$

Substituting the control into the dynamics for δ_4 leads to

$$\dot{\delta}_4 = \frac{k_1}{m} Q \delta_1 - \frac{k_1}{m} (k_2 I - Q) \delta_2 - \frac{(k_1 k_2 + k_3)}{m} \delta_3 - \frac{k_4}{m} \delta_4. \quad (32)$$

Consequently, choosing

$$S_4 := \frac{1}{2} |\delta_4|^2 \quad (33)$$

as the final storage function, one obtains

$$\dot{S}_4 = \frac{k_1}{m} \delta_4^T Q \delta_1 - \frac{k_1}{m} \delta_4^T (k_2 I - Q) \delta_2 - \frac{(k_1 k_2 + k_3)}{m} \delta_4^T \delta_3 - \frac{k_4}{m} \delta_4^T \delta_4 \quad (34)$$

From the above development present the following theorem.

Theorem 1 *Consider the dynamics defined by Eqn's 10-13. Let λ_{\min} and λ_{\max} be bounds on the maximal and minimal eigenvalues of Q . Let the vectorial controller be given by Eq. 31. Define the following candidate Lyapunov function*

$$\mathcal{L} = S_{1,2} + S_3 + S_4.$$

If the control gains satisfy

$$k_1 > 0, k_2 > \lambda_{\max}, k_3 > k_1 \lambda_{\max} \left(\frac{1}{\lambda_{\min}} + \frac{1}{k_2 - \lambda_{\min}} \right) \text{ and } k_4 > k_1 \left(\frac{\lambda_{\max}}{\lambda_{\min}} + \frac{k_2 - \lambda_{\min}}{k_2 - \lambda_{\max}} \right),$$

Then the Lyapunov function $\mathcal{L} \rightarrow 0$ converges asymptotically to zero.

The proof is a direct application of the principals of backstepping based on the development leading up the theorem statement. Note that the error coordinates δ_1 regulate the position of the camera. The error δ_2 regulates the linear velocity of the camera and ensures

¹This is possible for most systems but may fail for systems with a non-holonomic constraint.

that it comes to rest. The additional error coordinates δ_3 and δ_4 incorporate information on the orientation of the camera. If the position and linear velocity are regulated then the total external force must be zero, $F = 0$. Recalling Eq. 14 one has

$$R\mathbf{F} = e_3, \quad u = mg. \quad (35)$$

It follows that any rotation of the rigid body that would effect the orientation of \mathbf{F} is directly stabilized via the backstepping errors δ_3 and δ_4 .

5 Example

In this section the procedure presented in Section 4 is applied to an idealized model of the dynamics of an autonomous model helicopter.

An important control task for an autonomous helicopter is to locate and hover over a target. This task forms the first part of any landing manoeuvre. The position with respect to the target must be done relying on a local measurement system such as a visual system. The velocity V may be derived from a Kalman filter based on DGPS data and accelerometer data. The angular velocity Ω may be obtained by a 'three axis rate gyro' assembly while a three axis linear accelerometer, along with some basic filtering, will give a good approximation of the gravitational direction. Note that, the gravitational direction is the only inertial direction that is necessary for implementation of the proposed control.

An idealised dynamic model of a helicopter is considered where the motion of the airframe is modelled as that of a rigid object subject to a single force input, provided by the lift generated by main rotor collective pitch, and full torque control, derived from main rotor cyclic pitch and the tail rotor collective pitch. The dynamics of an observed target in the visual plane are given by Eqn's 10-13 with the force defined by

$$F = -ue_3 + mgR^T e_3 \quad (36)$$

where u is the force generated by the main rotor and e_3 is the body fixed direction in which the rotor is oriented. The value $R^T e_3$ is direction of gravity in the body fixed frame.

For the example considered the control law defined in Eq. 31 becomes

$$\left(\ddot{F} + \text{sk}(\dot{\Omega})F \right) = \left(-\ddot{u}e_3 + \text{sk}(\dot{\Omega})e_3 u \right) \quad (37)$$

Note that the second derivative of the heave control \ddot{u} enters into this expression. To implement the proposed design it is necessary to dynamically extend the heave control

$$\ddot{u} := v \quad (38)$$

where v is a new control input and the dynamics $\ddot{u} = v$ are computed within the control structure. Using the following transformation of Eq. 13,

$$w := -\mathbf{I}^{-1}\Omega \times \mathbf{I}\Omega + \mathbf{I}^{-1}\Gamma,$$

and knowing that $\text{sk}(e_3)$ is of rank two with entries only in the first and second columns one obtains

$$ve_3 + \text{usk}(\dot{\Omega})e_3 = \begin{pmatrix} uw^2 \\ -uw^1 \\ v \end{pmatrix} \quad (39)$$

It remains only to observe that as long as $u \neq 0$ the control signals w^1 , w^2 and v are uniquely determined by the visual servoing control Eq. 31. This is certainly be the case in hover conditions since $u \approx mg$ must counteract the gravitational force!

The above control design leaves $w^3 = e_3^T w$ free to stabilize the yaw angle to a desired value. In this example a simple proportional stabilizing feedback

$$w^3 := -K\Omega^3, \quad (40)$$

for $K > 0$ a suitable constant, is applied. Due to the decoupled nature of the rotation dynamics (using the transformed control w) one has

$$\frac{d}{dt}|\Omega^3|^2 = -K|\Omega^3|^2$$

and Lyapunov theory ensures that the yaw velocity converges to zero and that the helicopter (at least the one inside our computer) will stabilize in hover using visual data.

In the conference presentation some figures indicating the performance of the proposed design in simulation will be presented. Unfortunately, space restrictions prevent the authors from including these figures in the present paper. The performance in simulation is exactly as would be expected given the positive definite nature of the control Lyapunov function derived in the proposed design methodology.

References

- [1] B. Espiau, F. Chaumette, and P. Rives, "A new approach to visual servoing in robotics," *IEEE Transactions on Robotics and Automation*, vol. 8, no. 3, pp. 313–326, 1992.
- [2] S. Hutchinson, G. Hager, and P. Cork, "A tutorial on visual servo control," *IEEE Transactions on Robotics and Automation*, vol. 12, no. 5, pp. 651–670, 1996.
- [3] R. Pissard-Gibollet and P. Rives, "Applying visual servoing techniques to control of a mobile hand-eye system," in *Proceedings of the IEEE International Conference on Robotics and Automation, ICRA '95*, Nagasaki, JAPAN, 1995, pp. 166–171.
- [4] C. Samson, M. Le Borgne, and B. Espiau, *Robot Control: The task function approach*, The Oxford Engineering Science Series. Oxford University Press, Oxford, U.K., 1991.
- [5] P. Cork and M. Good, "Dynamic effects in visual closed-loop systems," *IEEE Transactions on Robotics and Automation*, vol. 12, no. 5, pp. 671–684, 1996.
- [6] R. Kelly, "Robust asymptotically stable visual servoing of planar robots," *IEEE Transactions on Robotics and Automation*, vol. 12, no. 5, pp. 759–766, 1996.
- [7] E. Zergeroglu, D. Dawson, M. de Queiroz, and S. Nagarkatti, "Robust visual-servo control of robot manipulators in the presence of uncertainty," in *Proceedings of the 38th Conference on Decision and Control*, Phoenix, Arizona, USA., 1999.
- [8] A. Maruyama and M. Fujita, "Visual feedback control of rigid body motion based on dissipation theoretical approach," in *Proceedings of the 38th Conference on Decision and Control*, Phoenix, Arizona, USA, 1999, pp. 4161–4166.
- [9] H. Zhang and J. P. Ostrowski, "Visual servoing with dynamics: Control of an unmanned blimp," in *Proceedings of the IEEE International Conference on Robotics and Automation*, Detroit, Michigan, U.S.A., 1999, pp. 618–623.
- [10] O. Shakernia, Y. Ma, T. J. Koo, J. Hespanha, and S. Sastry, "Vision guided landing of an unmanned air vehicle," in *Proceedings of the 38th Conference on Decision and Control*, Phoenix, Arizona, USA, 1999, pp. 4143–4148, Session FrA06.
- [11] M. Srinivasan, J. Chahl, K. Weber, S. Venkatesh, M. Nagle, and S. Zhang, "Robot navigation inspired by principles of insect vision," *Robotics and Autonomous Systems*, vol. 26, pp. 203–216, 1999.
- [12] R. Mahony, T. Hamel, and A. Dzul, "Hover control via approximate lyapunov control for a model helicopter," in *Proceedings of the 1999 Conference on Decision and Control*, Pheonix, Arizona, U.S.A., 1999.
- [13] M Krstic, I Kanellakopoulos, and P V Kokotovic, *Nonlinear and Adaptive Control Design*, American Mathematical Society, Providence, Rhode Island, U.S.A., 1995.
- [14] R. Mahony and T. Hamel, "Stable tracking control for unmanned aerial vehicles using non-inertial measurements," submitted to Conference on Decision and Control, 2000.
- [15] T. Hamel and R. Mahony, "Visual servoing of an under-actuated dynamic rigid-body system: An image based approach.," Submitted to IEEE Transactions on Automation and Robotics.